17th World Conference on Earthquake Engineering, 17WCEE
Sendai, Japan - September 27th to October 2nd, 2021

STUDY OF EFFECTS OF UNCERTAINTY IN GROUND MOTION AND SOIL PERMEABILITY ON CITYWIDE LIQUEFACTION USING HPC

J. Chen[(1)], H. O-tani [(2)], T. Takeyama[(3)], S. Oishi[(4)] and M. Hori[(5)]

[(1)] *Project Researcher, Japan Agency for Marine-Earth Science and Technology, jchen@jamstec.go.jp*
[(2)] *Research Scientist, RIKEN Center for Computational Science, h.o-tani@riken.jp*
[(3)] *Associate Professor, Kobe University, takeyama@people.kobe-u.ac.jp*
[(4)] *Professor, Kobe University, tetsu@phoenix.kobe-u.ac.jp*
[(5)] *Principal Researcher, Japan Agency for Marine-Earth Science and Technology, horimune@jamstec.go.jp*

Abstract

A physics simulation based approach for citywide assessment of liquefaction occurrence has been proposed recently as an alternative to the conventional engineering indices (EI-) based approach. In this approach, a finite element analysis model is constructed for a site where borehole data are available. A coupled soil-fluid analysis is then conducted for a presumed input ground motion. The occurrence of liquefaction is assessed by examining the computed excess pore water pressure (EPWP) from the dynamic simulation. Using high performance computing (HPC), a citywide assessment can be performed for an urban region with tens of thousands of sites. How to determine the material parameters for the soil constitutive models from the borehole data raises a concern about the uncertainty in soil parameters. The effects of soil parameter uncertainty on the liquefaction occurrence can be considered by conducting Monte-Carlo (MC) simulations with stochastically distributed model parameters for each site. In this paper, we apply MC simulations to study how the citywide liquefaction assessment is influenced by the changes both in the input ground motion and in the soil permeability. For studying the influence of input ground motion, a recorded ground motion in the great Hanshin earthquake is scaled and 100 MC models are constructed for each site with a varying soil permeability. This amounts to over 1 million MC models for the 10,000 plus sites in the target city. Both the dependence on the scale of the input acceleration and the variation due to the uncertainty in soil permeability are clarified. It is found out that with the increase of the scale of the input acceleration, the ratio of liquefied sites in the target city increases first and saturates eventually with an increasing error bar obtained from MC simulations. A comparison is made with the conventional method using the F_L index and it turned out that the assessment from the F_L index was considerably higher than the assessment from the physics simulation based approach, even considering the uncertainty in soil permeability with a scaled up input ground motion.

Keywords: liquefaction occurrence; citywide liquefaction assessment; soil uncertainties; soil dynamics analysis; Monte-Carlo simulations

1. Introduction

Liquefaction is a disastrous phenomenon that soil loses its shear strength and behaves like liquid because of the strong ground motion of an earthquake [1]. Earthquake disasters often introduce huge economic losses, among which liquefied soils cause significant and costly damage to residence buildings, civil structures and facilities. A study on the economic impact of earthquakes identified liquefaction as one of the main secondary-effect losses from historic worldwide earthquakes [2]. To enhance the preparedness before as well as the rapid response after major earthquakes, an effective and efficient prediction/assessment of the liquefaction hazard of an urban region is needed. How to further improve the effectiveness and efficiency of a citywide liquefaction hazard assessment is critical for liquefaction disaster mitigation.

The approaches to assess liquefaction hazard can be classified into two main categories: one approach is based on engineering indices (EI) and the other is based on soil dynamic analysis (SDA). Researches on liquefaction hazard assessment have been focused either on updating the fitting parameters or the formulas of EIs [3-7] for the former, or on refining constitutive models for high-fidelity simulations based on SDA [8-11] for the latter. In the EI-based approach, the occurrence of liquefaction for a site of interest is assessed based

on the load of earthquake and the resistance of the soil. Typical indices are the factor of safety of liquefaction (FS) and the liquefaction potential index (LPI), see e.g., Seed et al. [2]. In Japan, similar indices such as F_L and P_L are specified by Japan Road Association [12] as the standard liquefaction assessment approach. Due to its simplicity, the EI-based approach can assess the liquefaction hazard of a large urban region. Meanwhile, the SDA-based approach solves numerically the coupled governing equations for the motion of soils together with the changes of the excess pore water pressure (EPWP). The occurrence of liquefaction is then assessed based on the EPWP results according to the mechanism of liquefaction, viz., the increase of EPWP up to the level of overburden pressure. Since the construction of high-fidelity geometry and constitutive models for simulation is nontrivial, the application of SDA-based approach is often adopted for assessing liquefaction hazard for those individual sites of great importance, e.g., reservoir dams and river levees [8-11]. To take the advantage of the rigorousness of the SDA-approach for assessing liquefaction hazard for a city, the authors recently proposed to extend SDA-based approach for citywide liquefaction hazard assessment [13,14].

In comparison with the EI-based approach, the SDA-based approach possesses two major advantages: Firstly, the SDA-based approach takes into account EPWP directly to assess liquefaction occurrence. In contrast, neither the load parameter nor the resistance parameter in the EI-based approach is directly related to EPWP. Consequently, the EI-based approach cannot analyze the build-up of EPWP and its influence on the liquefaction occurrence assessment. Recurrence of liquefaction [15] or liquefaction due to aftershock [16,17] are such cases where the build-up of EPWP is critical for effective assessment of liquefaction hazard. Secondly, the SDA-based approach involves the input ground motion directly in simulations while the EI-based approach oversimplifies a seismic wave into one single parameter, e.g., the peak ground acceleration (PGA). It is well-known that two seismic waves of approximately the same PGA may introduce different levels of damages due the differences in frequency and in duration. Due to the above limitations, the assessment from the EI-based approach tends to overestimate liquefaction hazard. As can be seen from Table 1, a field survey after the 2011 Tohoku earthquake among 112 sites in Kanto region of Japan [18] showed that the false positive ratio was as high as 60%: 35 among 59 sites, which were not liquefied in the survey, were assessed as liquefied using F_L. Simulations [13] also showed that the number of sites being assessed as liquefied using F_L was about 1.5 to 2 times of the number from the SDA-based assessment.

Table 1 – Field survey and liquefaction assessment using F_L index for 112 sites in Kanto region after the 2011 Tohoku earthquake (original data refer to [18])

		Survey	
		Liquefied	Not-liquefied
Assessment	Liquefied: $F_L \leq 1$	53 (True Positive)	35 (False Positive)
	Not-liquefied: $F_L > 1$	0 (False negative)	24 (True Negative)

The authors proposed a new SDA-based methodology [13,14] for assessing citywide liquefaction hazard, in which SDA simulations are conducted for all the sites within a target urban region. In contrast to the common applications of SDA with high-fidelity models, our method adopted a strategy to combine a simple layered geometry with advanced soil constitutive models. This is a trade-off in site geometry that allows to assess many sites in a target city efficiently by taking advantage of the progress in high performance computing (HPC). As is seen in Fig. 1 (a), there are tens of thousands of sites within a target city to be assessed. From borehole logs and seismic records, simple layered finite element models can be constructed automatically for SDA simulations. We demonstrated that such automatized assessment can reproduce liquefaction for an individual site [19]. The simulation code has been parallelized for Monte-Carlo (MC) simulations of an individual site [20] and for assessing citywide liquefaction hazard of an urban region [13]. Efficient assessment can be conducted for tens of thousands of sites in urban regions, thanks to the development in HPC. Using such an HPC-empowered method, we also demonstrated a citywide probabilistic liquefaction assessment

considering the uncertainty in soil permeability [14]. As a continuing effort to further develop and demonstrate this new methodology, in this study we investigate quantitatively how the variations in input ground motion and the uncertainty in soil permeability influence the citywide assessment results. Due to the couplings of nonlinearity of soil dynamics and the uncertainty in soil permeability, a linear variation in the input ground motion is expected to result in a nonlinear variation in the citywide probabilistic assessment results. By using SDA-based assessment approach, we reveal quantitatively for the first time such input motion dependent citywide probabilistic assessment for liquefaction hazard.

The rest of the paper is organized as follows. Section 2 outlines the method and data used in this study. Section 3 presents the results from SDA simulations for a target city under different scenarios of varying input ground motions. Section 4 discusses the limitations of the present state of and possible future improvements for the SDA-based assessment approach, followed by concluding remarks in Section 5.

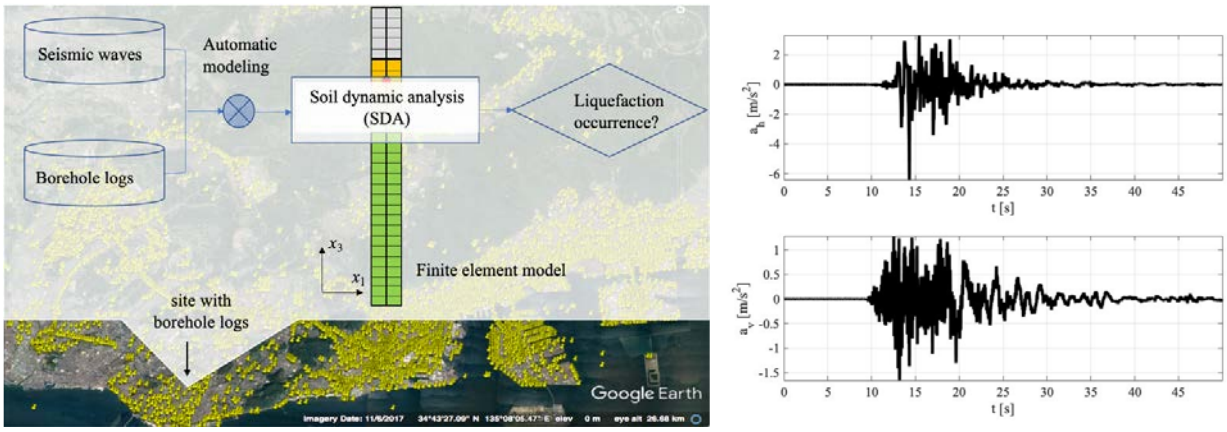

(a) (b)

Fig. 1 – (a) More than 10,000 sites with borehole logs (indicated by the yellow pins) within the target city, Kobe (Japan); (b) Input ground motion [21] as acceleration-time graphs from a seismic record of the 1995 Great Hanshin earthquake taken at Port Island of Kobe city (referred to as PI-wave in this paper).

2. Data and method

In this section, we explain briefly the data of the target city and the method for citywide liquefaction analysis. More details can also be found in previous publications [13,14,19,20].

2.1 Data of the target city

The target city in this study is Kobe city of Japan. Kobe is chosen for several considerations. Firstly, it has accumulated a database [22] of more than 10,000 pieces of borehole logs from various civil engineering projects. As is seen from Fig.1 (a), those sites with borehole logs cover almost the whole region of the target city except for the mountainous areas. A typical borehole log contains strata information, description of soil types, standard penetration test (SPT) *N* values, densities, and some logs also contain more information such as soil permeability and mechanic properties [19]. Secondly, this city was hit by a devastating earthquake in 1995, the Great Hanshin earthquake. This near-field earthquake not only introduced vast damages by the strong shaking directly but also caused a widely spread of liquefaction in the coastal areas featured by reclaimed lands [23]. The time histories of acceleration, as shown in Fig. 1 (b), used as input ground motion for liquefaction assessment were recorded by an array observation station [21] installed on an artificial island within the target city. The island, named Port Island (PI), suffered severe liquefaction due to this earthquake [23]. In this study, we used the wave record taken 83 meters below the ground level and referred to as PI wave for short. The PI wave will be used for all the sites in the target city. Ideally, the input ground motion should be site-dependent.

In practice, it is difficult to obtain such site-dependent information. Considering that the epic center is very near, it is valid to assume that the spatial variation is small for the sites within the target city. In this study, we scale the original PI wave linearly by k_s times to investigate the influence of input ground motion. The scale k_s ranges from 0.25 to 1.5 so that any possible spatial variations could be encompassed in the present study.

2.2 Governing equations and liquefaction criterion

For a given input ground motion, we conduct SDA for all the sites in the target city by solving the following governing equations,

$$\rho\ddot{\boldsymbol{u}} + \boldsymbol{\nabla}\cdot\boldsymbol{\sigma} - \rho\boldsymbol{b} = 0, \tag{1}$$

$$\dot{\varepsilon}_v + k\boldsymbol{\nabla}\cdot\boldsymbol{\nabla}p - \frac{n}{K_w}\dot{p} = 0, \tag{2}$$

to obtain the soil displacement $\boldsymbol{u}$ and EPWP p with auxiliary equations

$$\boldsymbol{\sigma} = \boldsymbol{\sigma}' + p\boldsymbol{I}, \tag{3}$$

$$\dot{\boldsymbol{\sigma}}' = \boldsymbol{C}:\dot{\boldsymbol{\varepsilon}}, \tag{4}$$

$$\boldsymbol{\varepsilon} = -\frac{1}{2}(\boldsymbol{\nabla u} + \boldsymbol{u\nabla}). \tag{5}$$

In the above equations, ρ, k, n, K_w stand for the soil density, permeability, porosity and pore water bulk modulus, respectively; $\boldsymbol{\sigma}, \boldsymbol{\sigma}', \boldsymbol{\varepsilon}, \boldsymbol{I}, \boldsymbol{C}, \boldsymbol{b}$ for the total stress tensor, effective stress tensor, strain tensor, identity tensor, constitutive tensor and body force, respectively; $\boldsymbol{\nabla}, \cdot, :, \dot{}, \ddot{}$ for the gradient operator, first order tensor contraction, second order tensor contraction, first order time derivative and second order time derivative, respectively. For a given input ground motion, e.g., Fig. 1 (b), the governing equations can be solved numerically with a constitutive model specified for the constitutive tensor $\boldsymbol{C}$. In this study, we adopted an extended Sekiguchi-Ohta model for describing the behaviors of saturated soils under cyclic loadings and applied the finite element method (FEM) to solve the governing equations [24]. Note that when the anisotropy parameter K_0 and contractancy parameter n_E are set as 1, the adopted constitutive model is reduced to the original Cam-clay model which is a typical soil constitutive model. Many other constitutive models have been proposed to reproduce liquefaction phenomenon [25]. Those models can also be implemented for citywide liquefaction hazard assessment. A different choice of constitutive model should not affect the citywide assessment result significantly.

By solving Eqs. (1-2) via FEM simulations, a time series of EPWP p(t) can be obtained. An EPWP ratio is defined as the maximum of p with respect to the effective overburden pressure σ_p'

$$r_p = \frac{\max(p)}{\sigma_p'}, \tag{6}$$

where σ_p' is the in situ mean effective stress. A soil layer is predicted as liquefied if its EPWP ratio exceeds a threshold ratio r_t

$$r_p \geq r_t. \tag{7}$$

Theoretically, $r_t = 1$ which means the overburden pressure is solely overcome by EPWP. In practice, soils became unstable when r_p is close to 1. We mainly set $r_t = 0.95$ as the liquefaction criterion based on an experimental study on the onset of liquefaction [26]. In literature, other threshold values were adopted, e.g., see [27]. The influence of r_t will also be examined in this study.

2.3 SDA-based citywide liquefaction hazard assessment

Figure 2 illustrates the methodology for citywide probabilistic liquefaction assessment: an automatic construction of numerical analysis models and an implementation of the SDA simulations on HPC platforms are two critical techniques to achieve citywide probabilistic assessment. The automatic model construction takes borehole logs and seismic records as input and generates SDA models as output. For a deterministic assessment, the soil parameters for SDA are estimated or determined from the information contained in borehole logs. In the previous study [19], we systematically summarized the equations which relate the soil properties in borehole logs to the soil parameters used for SDA simulations. To take into account the uncertainties, a probability distribution function (PDF) can also be specified to a soil property [14,20]. Note that for practical usages, the equations for parameter estimation in [19] must be calibrated with the experimental data of local soils. The SDA models are then solved numerically for the time series of EPWP. Based on EPWP results, the occurrence and consequently the hazard of liquefaction for an SDA model is assessed accordingly to Eq. (7). To efficiently simulate millions of SDA models, we parallelized the simulations on HPC platforms [14,20]. We demonstrated citywide probabilistic liquefaction assessment with the original PI wave [14]. In this study, we investigate how the interplay between the variation in input ground motion and the uncertainty in soil permeability will influence the probabilistic assessment results for the target city. The simulations for all the all the SDA models took less than 8 hours by using 4,096 computing nodes of the K computer, which was once ranked as the fastest supercomputer in 2011 and 2012 on the Top500 list (https://www.top500.org). Besides supercomputers, there are other options for an HPC implementation of the proposed methodology, such as using cost-effective General-Purpose Graphics Processing Units (GPGPUs).

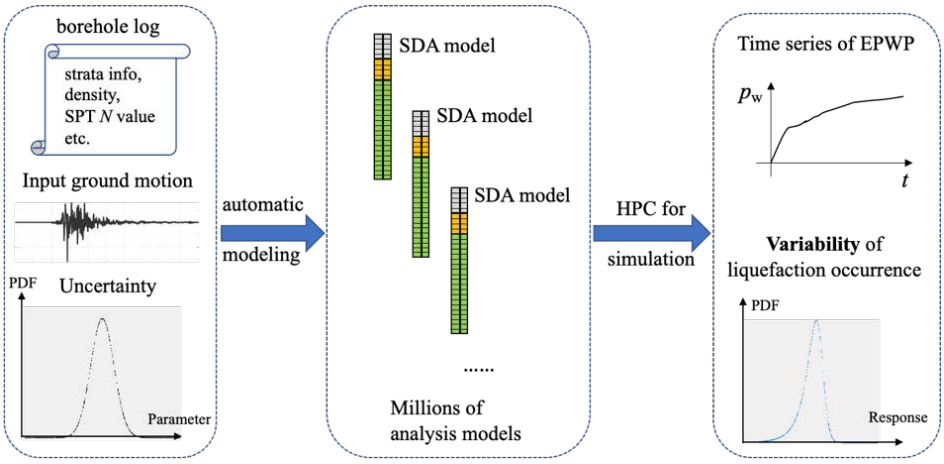

Fig. 2 – Schematic illustration of probabilistic liquefaction hazard assessment based on soil dynamic analysis (SDA): variations in input ground motion and uncertainties in soils are considered when constructing soil dynamic analysis (SDA) models; variability in liquefaction occurrence is measured from the simulation results for the excess pore water pressure (EPWP).

2.4 Monte-Carlo simulations for uncertainty

To take into account the uncertainties in soils, we employed the technique of Monte-Carlo (MC) simulations. For a soil property of interest, instead of specifying one deterministic value to construct one SDA model, we construct a certain number of SDA models for which the distribution of the parameter follows a given PDF. We demonstrated such MC simulations for a single site [19] and presented a probabilistic assessment for the target city using the original PI wave [14]. Similarly, the same MC models are constructed in this study for varying soil permeability k with a based-10-log-normal distribution. Considering that k varies among 2 to 3 orders for sand [28], the following distribution

$$\log_{10}(k) \sim \mathcal{N}(-4, 0.5), \tag{8}$$

is adopted for generating random values of k to construct SDA models. Eq. (8) specifies the exponent of k follows a normal distribution which is centered at -4 with a standard deviation as 0.5. Consequently, k has a mean value as 1×10^{-4} m/s which is a typical value for sand and 95% of the values of k lie in 1×10^{-3} m/s to 1×10^{-5} m/s. In this study, we construct 100 SDA models for one site with a random k which follows the distribution as in Eq. (8).

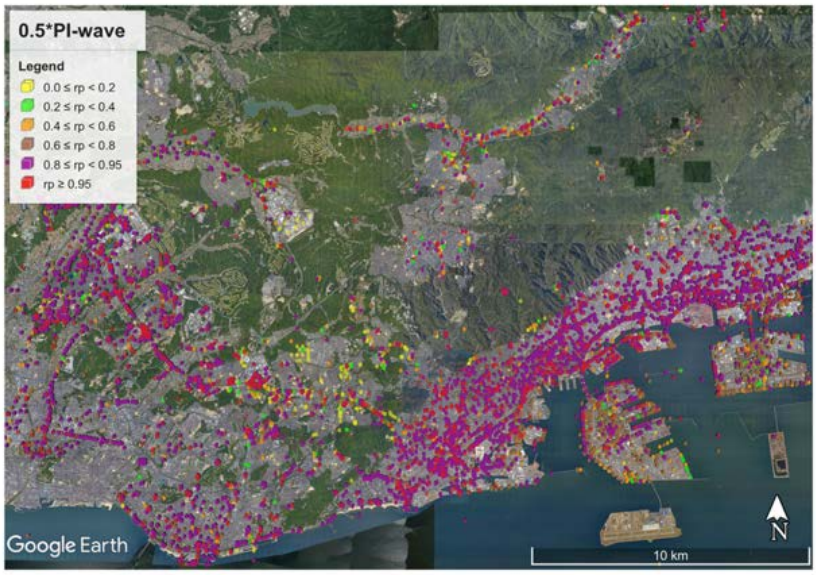

(a)

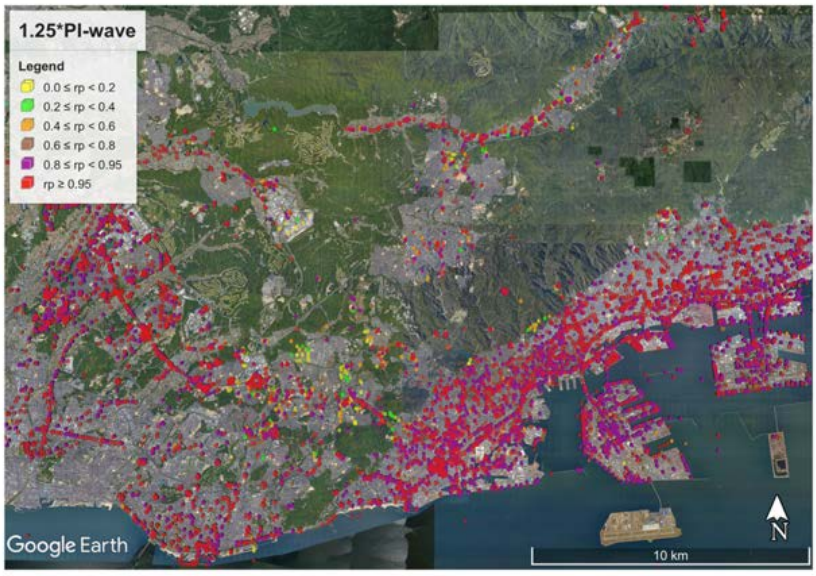

(b)

Fig. 3 – Citywide liquefaction hazard assessment with linearly scaled input ground motion of the original Port Island (PI-) wave: the median of r_p for each site is used for assessment with threshold $r_t = 0.95$. For 11,151 sites being assessed, the scaled-down scenario in (a) predicted 1,569 sites liquefied, while the scaled-up scenario in (b) predicted 4,701 sites liquefied.

3. Results

3.1 Citywide liquefaction hazard assessment

For each site, 100 MC models were constructed for SDA simulations. Based on the r_p of each MC mode, we obtained the probability of liquefaction hazard for each individual site. By chosen a representative statistic from the results of the 100 MC models of each site, we can further assess the citywide liquefaction hazard in a probabilistic sense. In Fig. 3, we demonstrate the results for two scaled input ground motion: the assessment results for a scaled down input ground motion by 50% is shown in Fig. 3 (a); the assessment results for an amplified input ground motion by 25% is shown in Fig. 3 (b). When the median of r_p was used as the representative statistic for each site, 1,569 sites liquefied in the scaled down case and 4,701 sites liquefied and in the scaled up case. As a comparison, a previous study predicted that 4,364 sites liquefied with the original PI wave [14]. The number of liquefied sites dropped more than 50% when we scaled down the PI wave by 0.5. In contrast, the number of liquefied sites increased less than 10% when we scaled up the PI wave by 1.25. This indicates a highly nonlinear influence on the liquefaction assessment from the input ground motion.

Besides the median, other statistics can be used to represent the liquefaction hazard of each site. For assessing citywide liquefaction hazard. In Fig. 4, we show the distribution of the EPWP ratio r_p when different representative statistics were chosen for the individual sites in the two scaled cases discussed above. For a threshold $r_t = 0.95$, the last bin in each histogram corresponds to the percentages of liquefied sites among the target city. In practice, the choice of representative statistics can be made according to the needs of liquefaction hazard assessment: while the median leads to a moderate prediction, the maximum and the minimum may be used for more conservative or aggressive prediction, respectively.

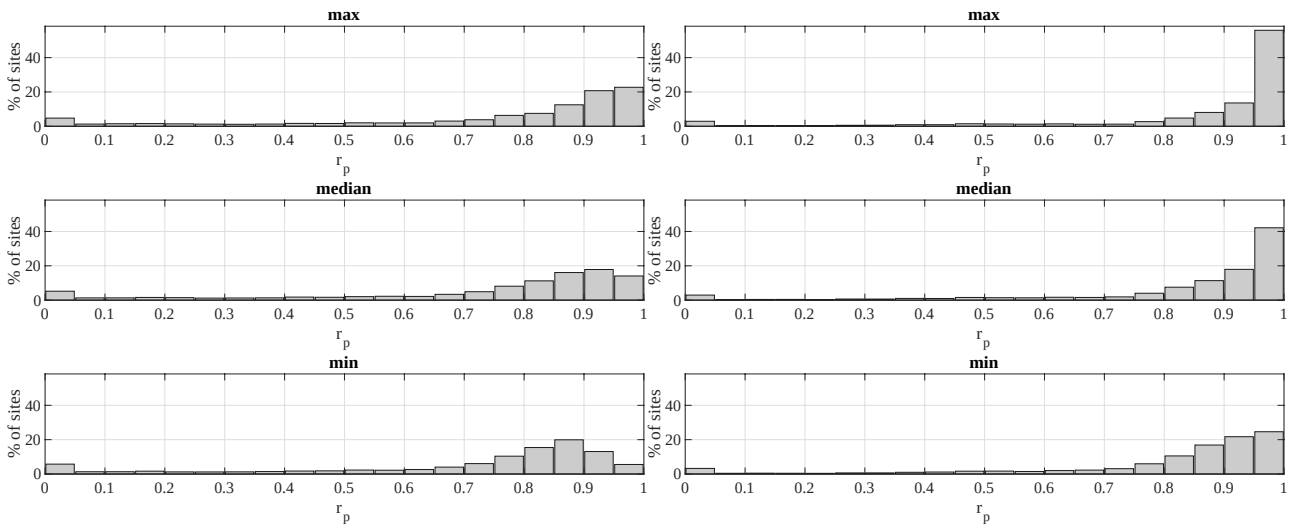

Fig. 4 – Citywide liquefaction hazard assessment with linearly scaled input ground motion of the original PI-wave: (a) scaled down with $k_s = 0.5$ and (b) scaled up with $k_s = 1.25$. The histograms show the distribution of r_p of three different representative statistics (the maximum, median and minimum).

3.2 Influence of input ground motion and permeability

To investigate the influence from the input ground motion, we scaled the original PI-wave with a linear factor k_s= {0.25,0.5,0.75,1.25,1.5} while k_s=1 corresponds to the original PI-wave. In Fig. 5 (a), we show the histograms for the median r_p of all sites for different k_s. When $k_s = 0.25$, it can be seen that the input motion resulted in a small median r_p for a majority of sites; when the input motion increased to $k_s = 0.5$, the induced r_p became larger and many sites had their median $r_p \geq 0.8$; when the input motion increased to 75% of the

original PI-wave, the liquefied sites (with $r_p \geq 0.95$ corresponding to the last bins in the histograms) turned out to be the largest category of r_p with a bin width as 0.05 in the histograms. A further increase of the input ground motion reduced the sites with moderate r_p to further expand the percentages of liquefied sites.

In Fig. 5 (b), we show how the percentage of liquefied sites η_L varies with respect to the scale factor k_s of the input ground motion. It can be regarded as an assessment with "error-bars", taking advantage of the various representative statistics from the MC simulations: the median is the main assessment; the error-bars from the minimum and the maximum prescribe the largest possible variations. More practically, the first and the third quartiles (Q1 and Q3, respectively) can serve as narrower error-bars. From Fig. 5 (b), the following observations can be made: 1) The percentage of liquefaction η_L varies nonlinearly with respect to k_s in such a way that the increase in the small range of k_s leads to a large increase in η_L and such increase in η_L becomes saturated when k_s is sufficiently large; 2) The width of the error bar, which is introduced by soil uncertainty, magnifies with respect to the scale factor of the input ground motion. In other words, for the same uncertainty in soil parameter, the larger the input motion, the larger the uncertainty in the assessment results. The saturation may be explained by the characteristics of the sites in the target city, i.e., the sites susceptible to liquefaction under this same type of input ground motion have been mostly identified via the large scale simulations.

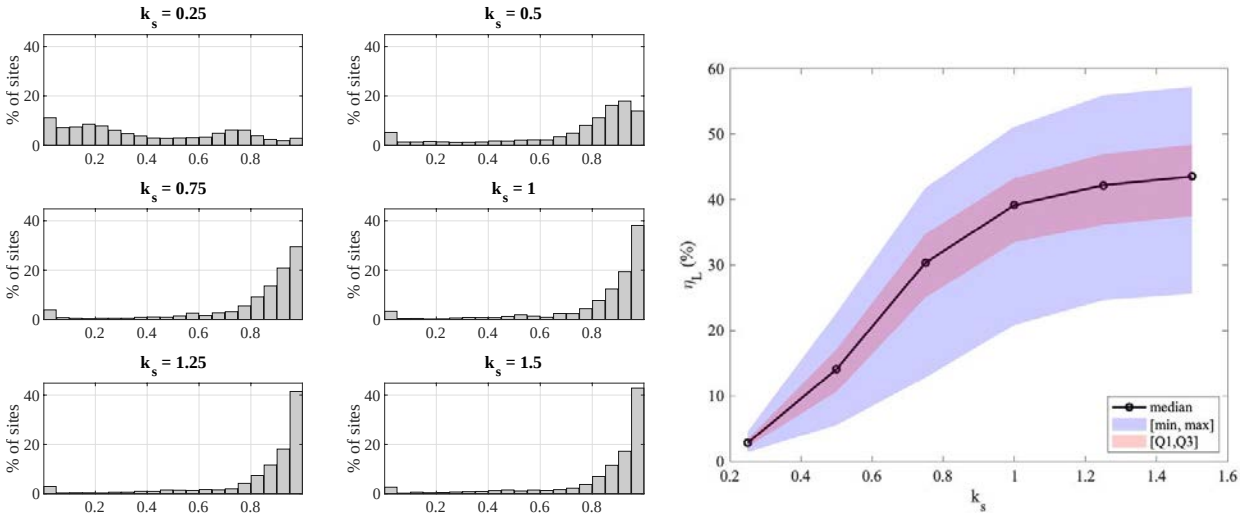

(a) (b)

Fig. 5 – Input ground motion dependent assessment results: (a) the distributions of r_p among all the sites of the target city with the median as the representative statistic for each site; (b) the percentage of liquefaction ($r_t = 0.95$) varies nonlinearly with respect to k_s, the scale factor of the input ground motion.

3.3 Influence of liquefaction threshold

From the previous study, it is known that by varying the threshold value r_t , the percentage of liquefied sites η_L changes nonlinearly for the original PI-wave [13]. From Fig. 6, it is clear now that the nonlinearity depends on the scale factor k_s of the input ground motion. In Fig. 6 we show how η_L varies with respect to r_t for different k_s, where η_L is assessed using the median r_p of each site. As is seen, when the input ground motion is small, $k_s \leq 0.5$, the variation with respect to r_t appears to be linear. When the input ground motion is large, $k_s \geq 0.75$, the nonlinear variation emerges and the curves for different k_s resemble. Besides the similar nonlinear variations, the convergence of η_L with respect to k_s observed in Fig. 5 (b) for $r_t = 0.95$ is also evident from Fig. 6 for different values of r_t. Especially, when $r_t < 0.95$, the difference between the assessment for $k_s = 1.25$ and for $k_s = 1.5$ become insignificant.

As a comparison, the assessment from the conventional F_L approach overestimates the liquefaction hazard of the target city. The assessment from F_L for the original PI-wave predicts liquefaction for a slightly

less than 90% of all the sites if the resistance of the soils were not adjusted ($c_1 = 1$). When the resistance to liquefaction is strengthened by setting $c_1 = 2$, about 66% of all the sites were assessed as liquefied using F_L. However, even we scaled up the original PI-wave by 1.5, which means 1.5 times of PGA for the EI-based assessment approach, the assessment from the median r_p did not exceed 60% with $r_t = 0.91$ and did not exceed 45% with $r_t = 0.95$. It is thus clear from this study that the conventional F_L approach do tend to overestimate liquefaction hazard for a citywide assessment, at least for earthquakes share the same characteristics of the recorded PI wave.

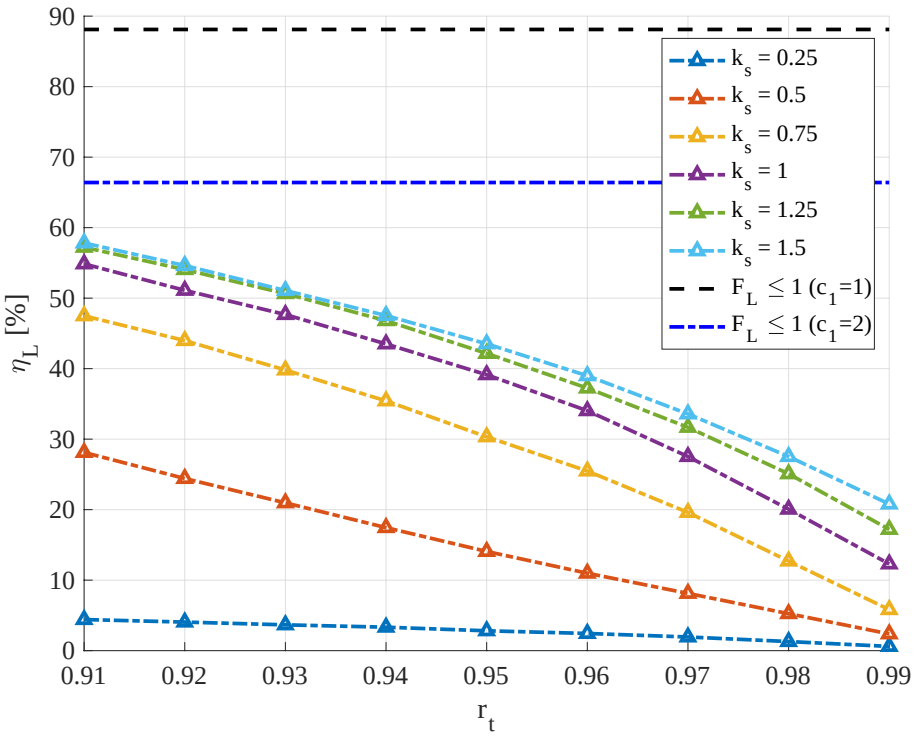

Fig. 6 – Influence of the liquefaction threshold r_t using the median r_p of each site to assess the percentage of liquefied sites η_L. The assessment results using F_L for the original PI-wave from [13] for comparison.

4. Discussion

This study is a continuing improvement for the SDA-based approach to assess citywide liquefaction hazard, as an alternative to the conventional EI-based approach. In this study, we showed that it is possible to obtain probabilistic assessment by considering the uncertainty in soil properties and the variation in ground motion together. To further improve the proposed approach for practical usages, several problems need to be addressed as future works.

The most critical problem is the evaluation of the accuracy of the assessment. To tackle this problem, we need verify and validate the simulation code [29]. While common validation involves comparison between high quality experimental data [30] and simulations of high-fidelity models. The error introduced in the simplification of high-fidelity models to 2D layered models should also be assessed. For practical use, field data from actual earthquakes should also be actively collected and compared for accuracy evaluation.

The uncertainty in ground motion is another important issue to be tackled. In this study, a near-field earthquake was investigated and the spatial variation of the seismic wave could be regarded as small. For far-field earthquakes, the spatial variation of the input ground motion should be taken into account. Although the same input ground motion is used for all the site in this study, the input acceleration has been linearly varied in a very large range. This large variation could cover the possible ranges of seismic uncertainty even for far-

field earthquakes. For far-field earthquakes, a random sampling among the simulation results in this study can provide a statistically meaningful liquefaction assessment to account for spatial seismic uncertainty. It is also possible to take into account directly the uncertainties in input ground motion by conducting MC simulations with varying input motions. In addition, there are also other methods, such as treating the seismic uncertainty as a problem of the evolution of probability density functions [31]. Those new methods can also be classified as SDA-based assessment approach, in which the fundamentals are the governing equations for soil dynamics. How to incorporate those new methods into the current SDA-based approach remains as a future work.

An advantage of SDA-based approach is that not only the EPWP results but also the surface motion of a site can be obtained. The massive data of the surface ground motion from simulations can be trained by neural networks [32] to make fast liquefaction assessment. This fast assessment is extremely useful after the occurrence of an earthquake, when the records of motion are available as input for the trained neural networks to obtain assessment in a few minutes. To further improve the assessment accuracy using neural networks trained by data generated from SDA-based approach is another interesting problem to address in the future.

5. Conclusion

In this study, we conducted SDA simulations for over 10,000 sites in a target city. For each site, 100 MC models were constructed and simulated to account for the uncertainty in soil permeability. For studying the influence of the variation in input ground motion, we further scaled the original PI-wave by a scale factor as 0.25, 0.5, 0.75, 1.25 and 1.5. It is found out that the assessment result based on the median of EPWP ratio r_p is highly nonlinear with respect to the input ground motion: the increase of r_p is fast when the input motion is small while a saturation is reached when the input ground motion is large. The error bars of the assessment, obtained from the statistics of MC simulations, amplifies as the input ground motion increases. When the input ground motion is relatively small, with a scale factor $k_\mathrm{s} \leq 0.5$, the assessment result varies linearly with respect to the liquefaction threshold value r_t. This trend becomes nonlinear when the input motion is large, when $k_\mathrm{s} \geq 0.75$. The convergence of the assessment is also observed for different choices of the threshold value r_t. The assessment from the conventional F_L index method for the original PI-wave is considerably larger in comparison with the SDA-based assessment for the input ground motion with 1.5 times of PI-wave. By further improving the accuracy and efficacy in future, the SDA-based assessment approach can serve as a promising alternative for the conventional EI-based approaches to assess citywide liquefaction hazard.

Acknowledgements

This research was supported by the FOCUS Establishing Supercomputing Center of Excellence.

References

[1] Kramer S (1996): *Geotechnical Earthquake Engineering*. Prentice-Hall.

[2] Daniell JE, Khazai B, Wenzel F, Vervaeck A (2012): The Worldwide Economic Impact of Earthquakes. In: *Proceedings of the 15th World Conference of Earthquake Engineering*, Lisbon, Portugal, Paper No. 2038.

[3] Poulos S, Castro G, France J (1985): Liquefaction evaluation procedure. *J. Geotech. Eng.*, **111**, 772–792.

[4] Seed RB, Cetin KO, Moss RES, Kammerer AM, Wu J, Pestana JM, Riemer MF, Sancio RB, Bray JD, Kayen RE, Faris A (2003): Recent advances in soil liquefaction engineering: A unified and consistent framework. In: *26th Annual ASCE Los Angeles Geotechnical Spring Seminar*.

[5] Kang GC, Chung JW, Rogers JD (2014): Re-calibrating the thresholds for the classification of liquefaction potential index based on the 2004 Niigata-ken Chuetsu earthquake. *Engineering Geology*, **169**, 30–40.

[6] Maurer BW, Green RA, Taylor ODS (2015): Moving towards an improved index for assessing liquefaction hazard:

Lessons from historical data. *Soils Found.* **55** (4), 778–787.

[7] Zhou YG, Xia P, Ling DS, Chen YM (2020): Liquefaction case studies of gravelly soils during the 2008 Wenchuan earthquake. *Engineering Geology*, **274**, 105691.

[8] Oka F, Yashima A, Shibata T, Kato M, Uzuoka R (1994): FEM-FDM Coupled Liquefaction Analysis of A Porous Soil Using an Elasto-Plastic Model. *Appl Sci Res*; **52**, 209–245.

[9] Zienkiewicz O, Chan A, Pastor M, Schrefler B, Shiomi T (1999): Computational geomechanics. Wiley.

[10] Ye B, Ye GL, Zhang F (2012): Numerical modeling of changes in anisotropy during liquefaction using a generalized constitutive model. *Computers and Geotechnics*, **42**, 62-72.

[11] Huang Y, Yashima A, Sawada K, Zhang F (2008): Numerical assessment of the seismic response of an earth embankment on liquefiable soils, *Bull Eng Geol Environ*, **67**, 31.

[12] Japan Road Association (2012): *Part V, Seismic Design, Specifications for Highway Bridges* (in Japanese).

[13] Chen J, O-tani H, Takeyama T, Oishi S, Hori M (2019): Toward a numerical-simulation-based liquefaction hazard assessment for urban regions using high-performance computing, *Engineering Geology*, **258**, 105153.

[14] Chen J, O-tani H, Takeyama T, Oishi S, Hori M (2021): A probabilistic liquefaction hazard assessment for urban regions based on dynamics analysis considering soil uncertainties, *Journal of Earth Science*, accepted.

[15] Wakamatsu K (2012): Recurrent Liquefaction Induced by the 2011 Great East Japan Earthquake, *Journal of Japan Association for Earthquake Engineering*, **12**(5), 5_69-5_88 (in Japanese).

[16] Yasuda S, Harada K, Ishikawa K, Kanemaru Y (2012): Characteristics of liquefaction in Tokyo Bay area by the 2011 Great East Japan Earthquake. *Soils Found.*, **52**(5), 793–810.

[17] Koyama T (2018): Chapter 8 - Liquefaction With the Great East Japan Earthquake. In: *The Fukushima and Tohoku Disaster: A Review of the Five-Year Reconstruction Efforts*. Butterworth-Heinemann, 147-159.

[18] The Japanese Geotechnical Society (2011): Soil liquefaction survey in Kanto district during the 2011 off the pacific coast of Tohoku earthquake. *Technical Report to Ministry of Land, Infrastructure, Transport and Tourism, Kanto Regional Development Bureau* (in Japanese).

[19] Chen J, Takeyama T, O-tani H, Fujita K, Hori M (2016): A framework for assessing liquefaction hazard for urban areas based on soil dynamics. *Int. J. Comput. Methods*, **13**, 1641011.

[20] Chen J, Takeyama T, O-tani H, Fujita K, Motoyama H, Hori M (2019): Using high performance computing for liquefaction hazard assessment with statistical soil models. *Int. J. Comput. Methods*, **15**, 1840005.

[21] Promotion Committee on Database of Strong Motion Array Observation (1998): *Tech. Rep. 3, Association for Earthquake Prevention*, Tokyo (in Japanese).

[22] Kobe-JIBANKUN Steering Committee (2013): *Web Kobe-JIBANKUN* (in Japanese).

http://www.strata.jp/KobeJibankun/.

[23] Shibata T, Oka F, Ozaka Y (1996): Characteristics of ground deformation due to liquefaction. *Special Issue of Soils and Foundations*, 65-79.

[24] Takeyama T, Tachibana S, Furukawa A (2014): A finite element method to describe the cyclic behavior of saturated soil. In: *Proceedings of the 2nd International Conference on Advances in Civil, Structural and Environmental Engineering*, 255–260.

[25] Hashiguchi K (2014): *Elastoplasticity theory*. Springer.

[26] Wu J, Kammerer AM, Riemer MF, Seed RB, Pestana JM (2004): Laboratory study of liquefaction triggering criteria. In: *Proceedings of 13th World Conference on Earthquake Engineering*, No.2580.

[27] Yoshida N, Sawada S, Nakamura S (2008): Simplified method in evaluating liquefaction occurrence against huge ocean trench earthquake. In: *Proceedings of 14th World Conference on Earthquake Engineering*, No.04-02-0011.

[28] Knappett JA, Craig RF (2012): *Craig's Soil Mechanics*. Spon Press, London.

[29] Chen J, Takeyama T, O-tani H, Oishi S, Hori M (2020): Code verification of soil dynamics simulations: A case study using the method of numerically manufactured solutions, *Computers and Geotechnics*, **117**, 103258.

[30] Manzari MT, Ghoraiby ME, Kutter BL, Zeghal M, Abdoun T, Arduino P, Armstrong RJ, Beaty M, Carey T, Chen Y, Ghofrani A, Gutierrez D, Goswami N, Haigh SK, Hung WY, Iai S, Kokkali P, Lee C-J, Madabhushi SPG, Mejia L, Sharp M, Tobita T, Ueda K, Zhou Y, Ziotopoulou K (2017): Liquefaction experiment and analysis projects (LEAP): summary of observations from the planning phase. *Soil Dyn. Earthq. Eng.*, **113**, 714–743.

[31] Huang Y, Xiong M, Zhou HB (2015): Ground seismic response analysis based on the probability density evolution method. *Engineering Geology*, **198**, 30–39.

[32] Bi CK, Fu B, Chen J, Zhao Y, Yang L, Duan Y, Shi Y (2019): Machine learning based fast multi-layer liquefaction disaster assessment. *World Wide Web*, **22**, 1935–1950.

